Evaluation of PETG mechanical behavior for application in vehicle protection

Gabriel Martins de Castro

Universidade de Brasília – campus Gama. Engenharia Automotiva

Rita de Cássia Silva

Universidade de Brasília – campus Gama. Engenharia Automotiva

Alessandro Borges de Sousa Oliveira

Universidade de Brasília – campus Gama. Engenharia Automotiva

ABSTRACT

During the last decades, highway authorities and motor vehicle manufacturers attempt to reduce the statistics of accidents in the world. However, the number of road traffic deaths continues to rise steadily, reaching 1.35 million in 2016. One of the accidents present in this statistic is the side-impact. Several researchers have dedicated themselves to develop passive safety devices that meet the demand for protection of the occupants in the event of collisions. Thin-walled energy absorbers are currently used to protect vehicle passengers against the harmful consequences of frontal collisions; though, the idea of using them against side impacts has not been appropriately explored. This work aims to present the experimental tests performed on the material PETG (polyethylene terephthalate glycol), a semicrystaline thermoplastic. The ASTM C365 covers the determination of compressive strength and modulus of sandwich cores, under quasi-static compressive loads. ASTM D638 reports the procedure to determine the tensile properties. The results draw that the material could have a significant contribution to resisting the impact, whether applied as a core of a thin-walled square mild-steel tube.

Keywords: Safety, PETG, Compression test, Tension test

INTRODUCTION

Energy-absorption systems are of considerable interest to automotive and aerospace engineering. During the years, many researchers have highlighted the effectiveness of these structures in dissipating impact energy by a stable progressive collapse mode when subjected to axial compressive loads.

Alghamdi (2001) [1] presented a review about thin-walled tubes demonstrating that these structures are the most widespread shape of collapsible impact energy absorbers. For this purpose, he showed about a hundred of references concerning this subject. Shindle and Mali (2018) [2] treated this topic focusing on the crushing behavior of energy absorbers covering about sixty-eight references related to metallic energy absorbers, and the application of composite tubes, fiber metal lamination (FML) member and honeycomb plate as a mean of impact protection.

The energy absorption capability of composite materials has mainly been studied in the last years. The research on composite materials has advanced because of their higher capacity of absorbing energy, adding low weight to the structure [3, 4]. The main composites identified to crash absorber are fiber-reinforced plastic (carbon fiber polymer [5], fiberglass [4, 6], and Kevlar [6], for instance) and foam (polyurethane [7], aluminum foam [8]). In terms of structural design, multi-cells thin-walled tubes have been performed better compared to single thin-walled tubes. Many researchers have indicated in their researches such a behavior [8, 9, 10]. However, its industrial production may not be simple to achieve [11]. Another way to improve the crashworthy ability of energy absorbers is to fill on the tubes with honeycomb structures [12]. These structures have the geometry of a honeycomb to minimize weight and cost. The geometry can vary, but the usual shape is hexagonal, forming hollow cells between thin plates.

The present work aims to present the experimental tests performed on the material PETG (polyethylene terephthalate glycol), a semicrystaline thermoplastic. The PETG composite is one of the most consumed material in 3-D printing fused deposition modeling method (FDM). This material presents a significant balance between strength and ease of printing. Besides, it has good shock resistance, and, in this work, it does not have any addition. Moreover, the PETG glass transition temperature is $T_g = 85°$. It represents the range of temperature where the polymer substrate changes from a rigid glassy material to a soft (not melted) [13]. The melting temperature is about 260°. Thus, at a temperature of 60° C, this polymer will be about 70% of its glass transition temperature, consequently, in its glassy

state. Above that, it becomes soft and more flexible, but not melted.

The ASTM C365/C365M [14] covers the determination of compressive strength and modulus of sandwich cores, under quasi-static compressive loads. ASTM D638 - 14 [15] reports the procedure to determine the tensile properties. The results draw that the material could have a significant contribution to resisting the impact, whether applied as a core of a thin-walled square mild-steel tube.

METHODOLOGY

A commercial filament of 1.75 mm of diameter was applied to print the specimens for both experimental tests in tension and compression. The printing speed, printing temperature and the platform temperature were 55 mm/min, 255º C and 70º C, respectively.

According to Chacón et al. [16], printing parameters have a considerable effect on the quality of the FDM printed parts, among them there are the build orientation, raster angle, infill density and layer thickness. Table 1 outlines the printing parameters adopted to the printing parts tested to tension in the present work.

Rodriguez-Panes et al. [17] estimated that infill percentage is the manufacturing parameter of greater relevance in the results and, depending on the material, it can have more or less influence.

Table 1 – Some printing parameters adopted to the tension specimens

Parameters	Values
Build orientation	Flat, on-edge
Raster angle	0º
Infill density	100%
Layer thickness	0.2 mm

The build orientation refers to how the sample is placed on the 3D printing platform, Fig. 2. In this work, two build orientations were considered flat and on-edge. Both had fused filament deposition in the loading tension direction.

Raster angle has been studied for many researchers as pointed out by [16, 17]. There is an agreement that this parameter strongly affects the anisotropy and strength of the pieces. For tensile tests, raster angle of 0º means that lines were oriented in the load direction. It is favorable to the specimen resistance.

Fernandez-Vicente et al. [18] studied the effect of pattern and density of infill in 3-D printing. The conclusions drawn that infill density affects the tensile strength. Actually, the value of 100% led to higher value of tensile strength in the pieces.

Rankouki et al. [19] concluded that smaller layer thickness increases the strength and, Caminero et al. [16] confirmed that in their work for flat and on-edge build orientations. They proposed layer thickness from 0.12 to 0.24 mm in order to have maximum tensile.

The specimens were tested in a servo-hydraulic machine with a loading capacity of 100 kN. The speed of testing was lower than those specified in the standard for samples of Type I (5 mm/min). Nevertheless, it produced a rupture below 5 min complying with item 8.2 of the standard.

Figure 1 illustrates the specimen placed in the testing machine. A dynamic extensometer 2620-601 was fixed in the 'G' length, as established by the standard.

Figure 1 – Specimen placed in the testing setup

The test specimens followed the dimensions described in the ASTM D638 [14], as Type I. Table 2 depicts the specimen in CAD and the main dimensions.

Table 2 – Dimensions and picture of the tensile specimen

Dimensions	Values
Width of narrow section (W)	13 mm
Length of narrow section (L)	57 mm
Distance between grips (D)	115 mm
Length overall (LO)	165 mm
Thickness (T)	3.2 mm
Width overall (WO)	19 mm

Five specimens were tested for two planes of anisotropy; 'xy' for the flat build orientation and 'yz' for the on-edge, as shown in Fig. 2. A cutoff at the center of 'L' length, Tab. 2, induced the failure in this region.
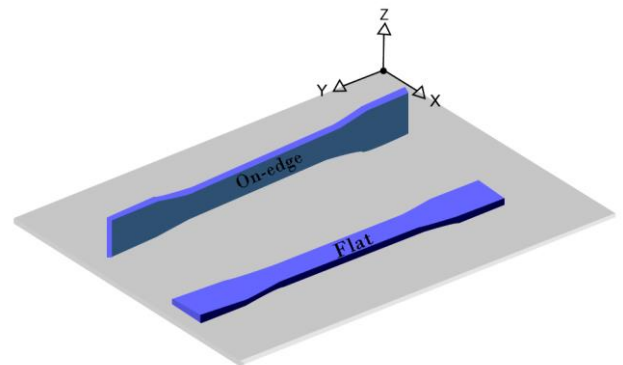
Figure 2 – Build orientation established for tension specimens

The tension testing allows determining four mechanical properties: flow stress, tensile strength at break, modulus of elasticity and elongation.

The standard test method [14] prescribes the experimental method to determine the compressive strength and modulus of sandwich cores. Notice that these properties are essential to the purpose of material using.

The aim of the experimental test was to determine the compressive response of the sandwich core under an out-of-plane loading tracking down the stress x strain curve. The out-of-plane direction presents the highest mechanical properties, as discussed in [20] and [21].

The parameters of interest related to the dimension of a honeycomb cell are cell angle, thickness, height and, length of the cell wall. These parameters were optimized to furnish a better performance against the compressive crushing.

Balaji et al. [22] and Meran et al. [23] observed that higher honeycomb density led to a larger mean crush force. It means that the honeycomb structure had thin cell thickness and a small length of the cell wall. Meran et al. [23] affirmed that the effectiveness in energy absorbing came from an adequate cell angle, where an angle of 120º yielded the largest energy absorbing. Contrary to the standard only three specimens were tested and, the samples were stabilized with thin facings. Specimens had a square cross-section and, the dimensions have complied with the Table 1 of the standard referring to the minimum and maximum cell size.

Table 3 presents the parameters adopted to the samples that were tested.
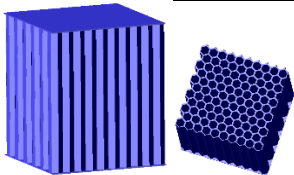
Table 3 – Some dimensions of the Sandwich core

Dimensions of honeycomb structure	Values
Density	260.7 kg/m^3
Cell angle	120º
Length of cell wall	3 mm
Thickness	0.4 mm

Table 4 outlines the printing parameters adopted to the printing parts tested to compression in the present work.

Table 4 – Some printing parameters adopted to the sandwich core specimens

Parameters	Values
Build orientation	Flat
Raster angle	90º
Infill density	100%
Layer thickness	0.4 mm

A pre-loading of 45 N acted on the samples and, the speed of testing was 3 mm/min, guaranteeing failure, as prescribed in the standard. Besides, the testing velocity ensured a quasi-static test.

The energy absorption capacity and the mean crushing loading allowed verifying the crashworthy ability of the honeycomb samples.

RESULTS

Figure 3 depicts the flat specimens after the test and, Figure 4 illustrates de on-edge specimens. The samples of both build orientation broke in the 'L' dimension, as prescribed by the ASTM standard.

During the on-edge specimens testing, two retests were carried out because a failure occurred in the limit of 'L' dimension and radius fillet. The failure mode was delamination, as discussed by [24] and [25].
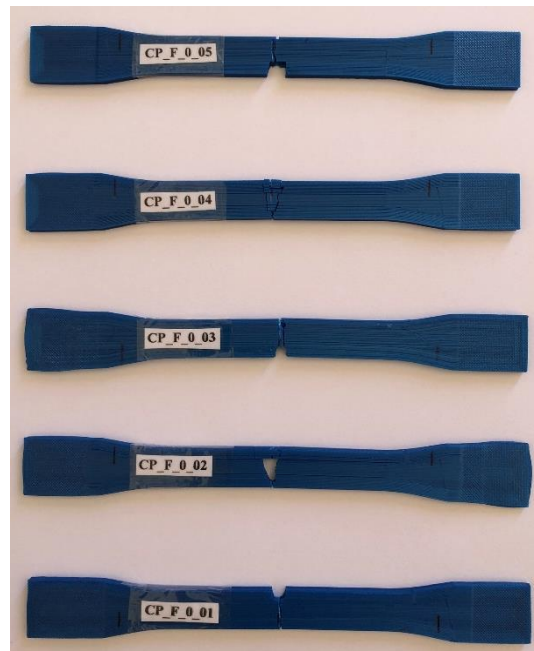

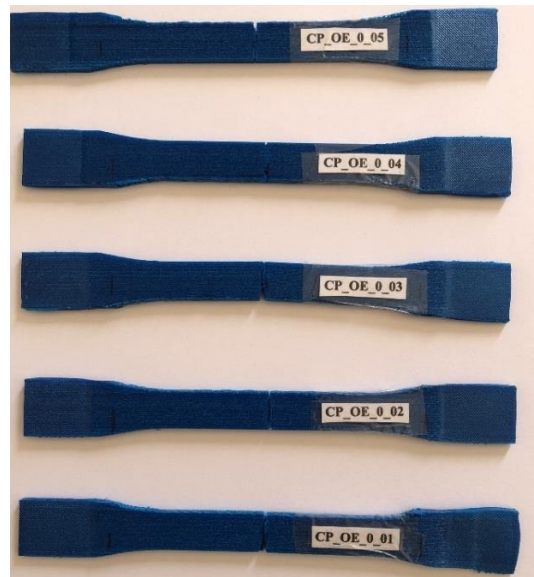Figure 3 – Flat specimens after the tension testing

Figure 4 – On-edge specimens after tension testing

All specimens failed as a rigid glassy material, independently of the build orientation mode, Fig. 5.
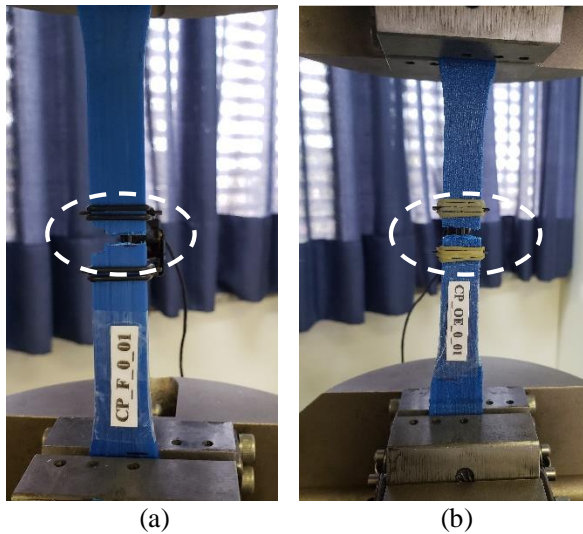
(a)   (b)

Figure 5 – Mode of failure of specimen according to the build orientation a) flat b) on-edge

Figure 6 and Figure 7 illustrates the curves of true stress versus true strain for the five samples designated, as CP_XX_YY_ZZ, where 'XX' refers to the adopted build orientation, 'YY' refers to the raster angle and 'ZZ' is the number of the sample.
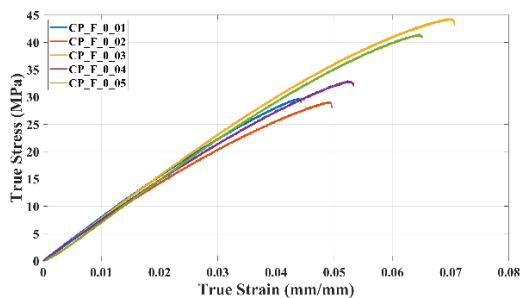

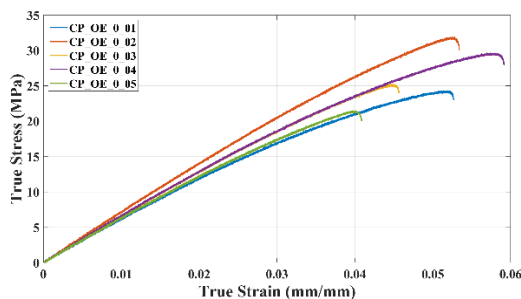Figure 6 – Curves true stress x true strain for the specimens flat

Figure 7 – Curves true stress x true strain for the specimens on-edge

Table 5 outlines the main results in tension, obtained for both build orientations. As discussed above, the selection of the FDM process parameters can interfere in the mechanical properties of the samples. The raster angle of 0° and the build orientations may maximize the values of stress because both led the fused filament to be put in the pull direction [16, 17].

The results corroborate those provided by one manufacturer; this way, the flow stress is 18.6 MPa, tensile strength at break 32.6 MPa, modulus of elasticity 1067.9 MPa and, elongation 7.7%. The most outstanding difference

between the values refers to the modulus of elasticity. It is worth noticing that the manufacturer did not inform the printing parameter.

The flow stress represents the offset yield point where a plastic strain of 0.5% occurred. In the present work, this value was adopted, as suggested by some researchers.

The tensile strength at break and the elongation were the values, in Fig. 6 and Fig. 7, where the sample failed.

Table 5 – Mechanical characteristics in tension for the specimens

Build orientation	Flat	On-edge
Flow stress (MPa)	29.8 ± 4.4	22.9 ± 2.9
Tensile strength at break (MPa)	30.8 ± 6.2	22.7 ± 3.8
Modulus of elasticity (MPa)	706.6 ± 27.4	611.8 ± 36.6
Elongation (%)	6.1 ± 1.2	5.4 ± 0.7

From the compressive testing concerning the honeycomb structures, Figure 8 depicts the sample after the crushing. Actually, uniform compressive failure of the sandwich core is the only acceptable failure mode. Notice that the failure of HC_01 and HC_03 outlines a shear due to the compression. The angle of the shear stress flow was about 35º for HC_01 and 25º for HC_03, both measured in the figure. The sample HC_02 did not have the same failure mode, apparently, the compression has led to a crushing mode.
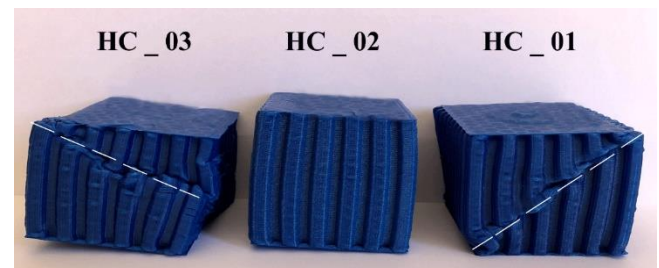

Figure 8 – Honeycomb structures after the compressive testing

Figure 9 outlines the curves for each compressed honeycomb. Notice that for HC_01 and HC_03 the stress suffers a considerably decrease followed by a constant stress. The shear stress flow seems to provoke an instability in the structure, as treated in [26, 27].
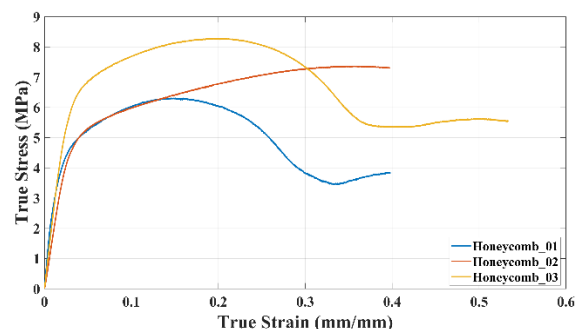

Figure 9 – Curves of true stress x true strain in compression loading

Table 6 summaries the main results obtained from the compression testing for each honeycomb specimen, as prescribed in the ASTM standard [14]. The mean crushing loading was estimated as a mean of determining the crashworthy ability of the material, as shown in Eq. 1.

$$P_m = \frac{E_{ab}}{\delta} \qquad (1)$$

where,

E_{ab} - from the curve compressive load versus compressive deflection; it represents the area under the curve;

δ - maximum deflection of the sample in m.

Table 6 – Mechanical characteristics in compression for each specimen

Mechanical characteristics	Honeycomb
Ultimate Strength (MPa)	9.6±1.9
Deflection Stress (kPa)	47.6±10.9
Compressive Modulus (kPa)	649.6±14.7
Crashworthy ability	
Energy absorption (J)	399.7±69.6
Mean Crushing Loading (kN) – Eq. 1	19.9±1.1
Mean Crushing Loading (kN) – Eq. 2 (considering [26] and [29])	6.6±0.5
Mean Crushing Loading (kN) – Eq. 2 (considering Tab.5)	8.4±0.5

The ultimate strength represents the maximum compressive capacity. The compressive modulus is defined as the slope of the linear region of the stress-strain curve. The suggested method [14] involves two-point slope calculation over the linear region of the force-displacement curve. The deflection stress reports to a specific value of strain about 2%.

An important factor to consider when investigating the performance of honeycomb core is its crushing strength [28] concerning the occupant safety. Wierzbicki [28] established a theoretical formulation to obtain the mean crushing loading of a cell of a honeycomb structure.

The method was based on the minimum principle in plasticity and energy considerations, which took into account the parameters of the cell wall thickness (t), the width of the cell wall (l), and the flow stress (σ_0) of the material used. The mean crushing loading was given, as illustrated in Eq. 2.

$$P_m = 8.61 \sigma_0 \, t^{5/3} (1/l^3) \qquad (2)$$

Equation 2 shows that the mean crushing loading depends on the flow stress (σ_0). Over the decades, a number of studies about this prediction were developed as treated in the work of McFarland [26]; and Magee and Thornton [29]. Thus, Wierzbicki [28] affirmed that when considering theoretical and experimental results obtained in honeycomb experiments; the correlation between the flow stress and the

ultimate strength, $\sigma_0 = 0.7\sigma_u$, seemed to be adequate and closely follows the trend of the tests points. Thus, in the present work, the mean crushing loading was estimated following the results of [26, 29] and using the stress found experimentally for the flat sample, Tab. 5.

The results of the mean crushing loading showed that the value assessed by Eq. 1 is higher than the other two. It is worth noting that the formula does not depend on any mechanical property of the material; it involves concepts of work and energy transformation when calculating the energy absorption. Besides, the maximum deflection was about 20 mm.

The mean load value estimated by Eq. 2 became a little more realistic when considering the flow stress determined through the tension experiments. The values in Tab. 6 the mean crushing load estimated for one cell multiplied by the number of them in the sandwich. Thus, the results could be underestimated by using the proposed formula.

CONCLUSIONS

The standards of ASTM are adequate to determine the main properties for composite structures. For the experimental tension tests, the properties values comply with those provided by a manufacturer, except the modulus of elasticity. The build orientation in flat leads to higher values of mechanical properties.

The compressive experimental tests furnished the mechanical characteristics expected in the standard. Based on these tests, the authors also investigated the crashworthy ability of the material, determining the mean crushing load and energy absorption. Three values are obtained for the mean crushing loading. The first correspond to a performance indicator where the mean force is determined from the energy absorption, Eq. 1. The others are obtained from a theoretical formulation found in the technical literature varying the way as the flow stress is considered.

From the results of crashworthy ability relative to the mean crushing loading, authors considered that Eq. 1 is the best way to estimate this performance indicator. The reason is that the formula does not depend on any mechanical property of the material; it involves concepts of work and energy transformation when calculating the energy absorption. Also, it is directly determined from experimental data.

This way, it seems that the PETG filament may be tested for application in vehicle protection due to its capacity of absorbing energy and mechanical properties, as shown in the present work.

ACKNOWLEDGMENTS

REFERENCES

[1] Alghamdi, A., 2001. Collapsible impact energy absorbers: an overview. Thin-walled structures, Elsevier, vol. 39, n. 2, pp. 189–213.

[2] Shindle, R. B., Mali, K. D., 2018. An overview on impact behavior and energy absorption of collapsible metallic and non-metallic energy absorbers used in δ applications. IOP Conf. Ser.: Mater. Sci. Eng. 346 012054.

[3] Mantovani, S., Cavazzuti, M. and Torricelli, E., 2011. Lightweight crash energy absorber design using composite materials. Int. Conf. on Mech., Aut. And Aerosp. Eng.

[4] Ruzicka, M., Kulisek, V., Bogomolov, S. and Shánel, V., 2014. Development of composite energy absorber. Procedia Engineering, vol. 96, pp. 392-399.

[5] Guida, M., Marulo, F., Bruno, M., Montesarchio, B. and Orlando, S., 2018. Design validation of a composite crash absorber energy to an emergency landing. Adv. In Airc. And Spacecraft Sc., vol. 5 n°. 3, pp. 319-334.

[6] Thornton, P. H., Harwood, J. J. and Beardmore, P., 1985. Fiber-reinforced plastic composites for energy absorption purposes. Composites Science and Technology 24, pp. 275-298.

[7] Patel, J. and Stojko, S., 2010. Characterizing polyurethane foam as impact absorber in transport packages, Packaging, Transport, Storage & Security of Radioactive Material, 21:1, 25-30

[8] Zhang, X. and Cheng, G., 2007. A comparative study of energy absorption characteristics of foam-filled and multi-cell square columns. Int, J. of Imp. Eng., vol. 34, pp. 1739-1752.

[9] Alavi Nia, A. and Parsapour, M., 2013. An investigation on the energy absorption characteristics of multi-cell square tubes. Thin-Walled Structures, 68, 26–34.

[10] Hussein, R. D., Ruan, D., Lu, G., Guillow, S. And Yoon, J. W., 2017. Crushing response of square aluminum tubes filled with polyurethane foam and aluminum honeycomb. Thin-Walled Structures, vol. 110, pp. 140-154.

[11] Baroutaji, A., Sajjia, M. And Olabi, A. G, 2017. On the crashworthiness performance of thin-walled energy absorbers: Recent advances and future developments. Thin-Walled Structures, vol. 118, n. April, p. 137–163. DOI: http://dx.doi.org/10.1016/j.tws.2017.05.018.

[12] Zarei, H. and Kroger, M., 2008. Optimum honeycomb filled crash absorber design. Materials and Design 29, pp. 193-204.

[13] Becker, H. and Locascio, L. E., 2002. Polymer microfluidic devices. Talanta, vol. 56, pp. 267-287.

[14] ASTM C365/C365M – 16, 2016. Standard test method for flatwise compressive properties of sandwich cores. American Society for Testing and Materials.

[15] ASTM D638 – 14, 2014. Standard test method for tensile properties of plastics. American Society for Testing and Materials.

[16] Chacón, J.M., Caminero, M. A., Garcia-Plaza, E. and Nunez, P. J., 2017. Additive manufacturing of PLA structures using fused deposition modelling: effect of process parameters on mechanical properties and their optimal selection. Doi: 10.1016/j.matdes.2017.03.065.

[17] Rodriguéz-Panes, A., Claver, J. and Camacho, A.M, 2018. The influence of manufacturing parmeters on the mechanical behavior of PLA and ABS pieces manufactured by FDM: a comparative analysis. Material, vol. 11, pp. 1333. DOI: 10.3390/ma1081333.

[18] Fernandez-Vicente, M., Calle, W., Ferrandiz, S. and Conejero, A., 2016. Effect of infill parameters on tensile mechanical behavior in desktop 3D printing. 3D printing and additive manufacturing, vol. 3, n° 3, pp.183-192. DOI: 10.1089/3dp.2015.0036.

[19] Rankouhi B., Javadpour S., Delfanian F. and Letcher T., 2016. Failure analysis and mechanical characterization of 3D printed ABS with respect to layer thickness and orientation. J. Fail. Anal. Prev., vol.16, pp. 467–481.

[20] Zhao, H., Gary, G., 1998. Crushing behavior of aluminium honeycombs under impact loading. International Journal of Impact Engineering, vol. 21, n. 10, p. 827-836.

[21] Khan, M. K., Baig, T., Mirza, S., 2012. Experimental investigation of in-plane and out-of-plane crushing of aluminium honeycomb. Materials Science and Engineering A, vol. 539, p. 135-142. DOI: 10.1016/j.msea.2012.01.07

[22] Balaji, G. and Annamalai, K., 2018. Numerical investigation of honeycomb filled crash box for the effect of honeycomb's physical parameters on crashworthiness constants. International Journal of Crashworthiness, DOI:10.1080/13588265.2018.1424298.

[23] Meran, A. P., Toprak, T. and Mugan, A., 2014. Numerical and experimental study of crashworthiness parameters of honeycomb structures. Thin-Walled Structures, vol. 18, pp. 87-94.

[24] Jap, N. S. F. and colab., 2019. The effect of raster orientation on the static and fatigue properties of filament deposited ABS polymer. International Journal of Fatigue, vol. 124, n. February, p. 328-337. DOI: https://doi.org/10.1016/j.ijfatigue. 2019.02.042.

[25] Ziemian, C., Sharma, M., Ziemian, S., 2012. Anisotropic Mechanical Properties of ABS Parts Fabricated by Fused Deposition Modelling. Mechanical Engineering, Dr. Murat Gokcek (Ed.). ISBN: 978-953-51-0505-3.

[26] McFarland, R. K., 1963. Hexagonal Cell Structures Under Post-Buckling Axial Load. AIAA Journal, vol. 1, n. 6, p. 1380-1385. DOI: https://doi.org/10.2514/3.1798.

[27] Jin, T., Zhou, Z., Wang, Z., Wu, G., Shu, X., 2015. Experimental study on the effects of specimen in-plane on the mechanical behavior of aluminum hexagonal honeycombs. Materials Science and Engineering A, vol. 635, p. 23-35. DOI: 10.1016/j.msea.2015.03.053.

[28] Wierzbicki, T., 1983. Crushing Analysis of Metal Honeycombs. International Journal of Impact Engineering, vol. 1, n. 2, p. 157-174.

[29] Magee, C. L., Thornton, P. H., 1978. Design Considerations in Energy Absorption by Structural Collapse. SAE Technical Papers. DOI: https://doi.org/10.4271/780434.